Biochemical and Biophysical Research Communications 743 (2025) 151159

Contents lists available at ScienceDirect

Biochemical and Biophysical Research Communications

journal homepage: www.elsevier.com/locate/ybbrc

Evaluation of the digestion protocol of mouse neonatal epidermis for single-cell RNA sequencing

Asaka Miura [a], Tomomi Kitayama [b], Yuya Ouchi [b], Kotaro Saga [a], Takashi Shimbo [a,c,*], Katsuto Tamai [a,b,**]

[a] Department of Stem Cell Therapy Science, Graduate School of Medicine, Osaka University, Suita, Japan
[b] StemRIM Inc., Ibaraki, Osaka, Japan
[c] StemRIM Institute of Regeneration-Inducing Medicine, Osaka University, Suita, Japan

ARTICLE INFO

Keywords:
Skin
Transcriptomics
Single-cell transcriptome
Keratinocytes

ABSTRACT

The skin is primarily composed of keratinocytes and forms an effective barrier between the organism and external environment. Neonatal skin analysis is essential for understanding developmental processes and rare skin diseases. However, efficient single-cell dissociation methods for the neonatal mouse epidermis remain underexplored. Here, three enzymes (Trypsin, TrypLE, and Liberase) used for tissue dissociation were compared to optimize single-cell RNA sequencing (scRNA-seq) of the mouse neonatal epidermis. scRNA-seq revealed distinct differences in cell recovery between the enzymes, with Liberase enriching suprabasal keratinocytes and Trypsin/TrypLE favoring basal keratinocytes. Although all enzymes produced comparable data quality, the observed bias in cell population recovery highlights the significant impact of dissociation protocols on the scRNA-seq results. These findings highlight the importance and optimal selection of enzymes for the analysis of unbiased neonatal epidermis.

1. Introduction

The skin is a multilayer organ that serves as a barrier at the interface between the organism and external environment [1]. The outer layer of the skin is called the epidermis, is primarily composed of keratinocytes. The basal layer is the innermost layer of the epidermis and acts as the starting point for keratinocyte supplementation [2]. The intermediate layers constitute the spinous layer, which contains actively dividing keratinocytes; granular layer, which plays a pivotal role in skin barrier function by forming tight junctions [3]; and the outermost stratum, corneum, that is responsible for water retention and prevents entry of foreign substances [4]. Although the skin is primarily composed of keratinocytes, it exhibits highly specialized and unique characteristics.

Skin abnormalities can lead to various diseases. Genetic mutations in type VII collagen, a component of the basement membrane, result in recessive dystrophic epidermolysis bullosa [5,6], while mutations in genes such as ATP-binding cassette transporter subfamily A member 12 (ABCA12) cause autosomal recessive congenital ichthyosis [7]. Symptoms of these conditions manifest on the skin immediately after birth, highlighting the importance of an in-depth analysis of neonatal skin to better understand these rare diseases and develop novel therapeutic approaches.

Recently, single-cell RNA sequencing (scRNA-seq) has been widely used to understand skin physiology and pathology. To obtain high-quality data, a sophisticated method for converting skin into a single-cell suspension is essential. The method must be able to digest tissues without damage or bias. Although such methods for human skin tissue [8] and adult mouse skin [9,10] have been established, methods for neonatal mouse skin is limited. Therefore, this study aims to investigate and compare multiple conversion methods to obtain single-cell suspensions from neonatal skin of mice.

2. Materials and methods

2.1. Animal models

All animal handling procedures were conducted in accordance with the protocols and guidelines approved by the Animal Committee of the

* Corresponding author. Osaka University Graduate School of Medicine 2-2, Yamadaoka, Suita, Osaka, 565-0871, Japan.
** Corresponding author. Osaka University Graduate School of Medicine 2-2, Yamadaoka, Suita, Osaka, 565-0871, Japan.
E-mail addresses: shimbot@sts.med.osaka-u.ac.jp (T. Shimbo), tamai@gts.med.osaka-u.ac.jp (K. Tamai).

https://doi.org/10.1016/j.bbrc.2024.151159
Received 7 December 2024; Accepted 9 December 2024
Available online 10 December 2024

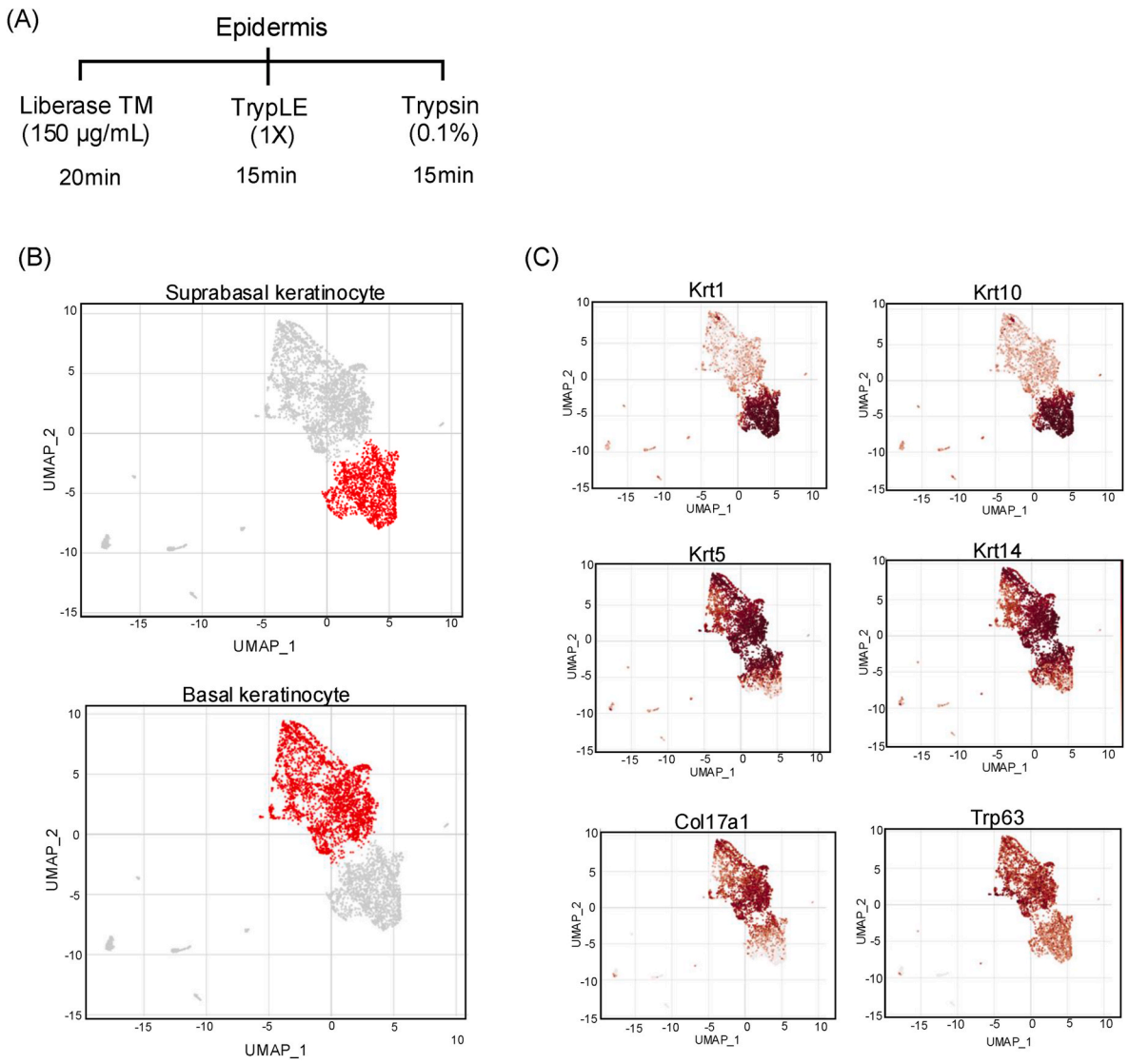

Fig. 1. (A) Experiment overview. (B) UMAP plots showing two main clusters, suprabasal keratinocytes and basal keratinocytes. (C) UMAP plots showing the expression distribution of epithelial genes.

Osaka University Graduate School of Medicine. The following mouse strains were generated and obtained from Jackson Laboratory (West Grove, PA, USA): Pdgfra^{EGFP} (B6.*129S4-Pdgfratm11(EGFP)Sor/J*) [11], Pdgfra^{Cre} (C57BL/6-Tg*(Pdgfra-cre)1Clc/J*) [12], Ai9 (B6.Cg-*Gt(ROSA)26Sortm9(CAG-tdTomato)Hze/J*) [13] and Pdgfra^{EGFP}; Pdgfra^{Cre}; ROSA^{tdTomato}.

2.2. Mouse tissue cell preparation

Epidermal and dermal fibroblasts from the head were collected separately. The skin was soaked in a solution containing 2,000 PU/mL DISPASEII (FUJIFILM Wako, Osaka, Japan) at 4 °C overnight. Subsequently, the epidermis and dermis were separated and washed with Minimum Essential Medium alpha (MEMα) (Thermo Fisher Scientific, Waltham, MA, USA) supplemented with 2 % fetal bovine serum (FBS). To identify the ideal enzyme for mouse neonatal epidermis digestion, three common enzymes, Trypsin [10], TrypLE [14], and Liberase [15,16], were selected and used for tissue processing. Each sample was minced and then incubated with 2–3 mL of TrypLE Select (1X; Thermo Fisher Scientific), 0.1 % Trypsin, and 150 μg/mL Liberase TM Research Grade (Thermolysin Medium) (Merck, Rahway, NJ, USA). The concentration of Trypsin (0.1 %) was adjusted by diluting trypsin-EDTA (0.25 %; Thermo Fisher Scientific) with Dulbecco's phosphate-buffered saline (Nacalai Tesque, Kyoto, Japan) immediately before digestion. Each enzyme buffer was supplemented with 10 U of DNaseI (Takara, Shiga, Japan). After incubation in a 37 °C water bath (15–20 min for TrypLE and Trypsin; 20–30 min for Liberase), the cell supernatant was pipetted with an additional 3 mL of RPMI1640 (NACALAI TESQUE, Kyoto, Japan) buffer containing 5 % FBS, which was then collected and centrifuged at 300 *g* for 5–10 min. The remaining pellet was then suspended in 200 μL of MEMα supplemented with 2 % FBS.

2.3. Plate-sorting-based single-cell RNA-seq in mice

To ensure accurate sorting for scRNA-seq, dead cells were identified by staining with SYTOX™ Blue Dead Cell Stain (Thermo Fisher Scientific) immediately before sorting. Target cells were sorted using a BD FACSAria III instrument (BD Biosciences, NJ, USA). The scRNA-seq protocol was performed as previously described, with minor modifications [17]. Briefly, 1 ng of amplified cDNA was used for titration, and libraries were sequenced on a NextSeq 2000 platform (Illumina, San Diego, CA).

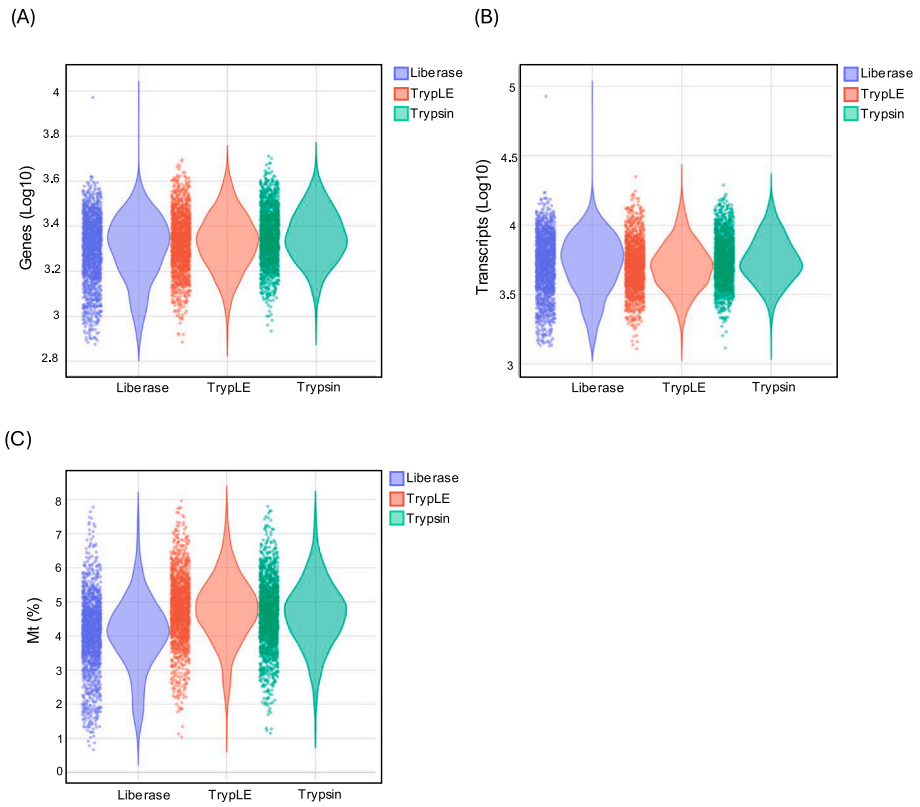

Fig. 2. (A) The number of genes per cell. (B) The number of transcripts per cell. (C) The percentage of mitochondrial genes.

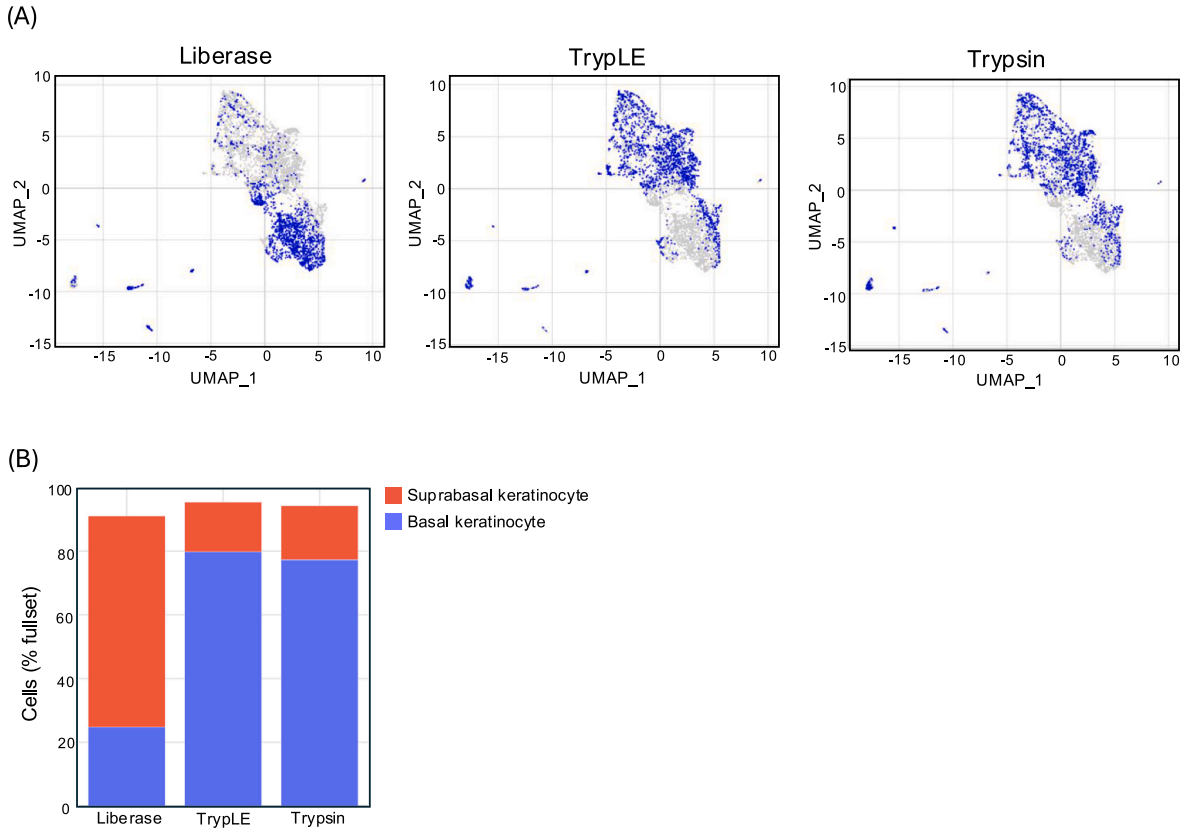

Fig. 3. (A) UMAP plots showing comparison of the cell distribution in each cluster across enzyme process (Liberase, 1466 cells; TrypLE, 1519 cells; Trypsin, 1454 cells).
(B) Bar charts showing the proportions of suprabasal and basal keratinocytes depending on enzyme treatment.

2.4. Bioinformatics

Sequence outputs were demultiplexed using bcl2fastq [18] and cell ranger mkfastq [19] for plate sorting and droplet-based scRNA-seq, respectively. For bcl2fastq, the following options were used: use-bases-mask Y20, I8, I8, Y50n, no-lane-splitting, minimum-trimmed-read-length 20, and mask-short-adapter reads. Demultiplexed fastq files were aligned to the mm10 or GRCh38 genome using STAR aligner (2.7.3a) [20] and CellRanger count for plate sorting and droplet-based scRNA-seq, respectively. STAR was performed with-soloType CB_UMI_Simple,-soloFeatures Gene,-soloUMI filtering, and MultiGeneUMI options, and the soloCBwhitelistSTARsolo output matrix was merged and analyzed. CellRanger analysis was performed using default options. The aligned count data were analyzed using the Seurat package [21]. Marker genes for each cell cluster were identified using the Seurat FindAllMarkers function with the default options. Differential gene expression was analyzed using the Seurat FindMarkers function with the test option. Gene Ontology (GO) enrichment analysis was performed and visualized using clusterProfiler [22,23] and enrichplot [24]. Uniform Manifold Approximation and Projection (UMAP), gene expression, and other sequencing data were visualized using the Plotly package [25] and ggplot2 [26].

3. Results

Trypsin is a well-known serine endopeptidase and TrypLE is a recombinant trypsin-like proteinase that is gentle to cells. Liberase is a mixture of collagenases I and II, and thermolysin. Briefly, the epidermis was detached by treatment with Dispase II. Digestion of the epidermis with each enzyme was conducted under common conditions for each enzyme (Fig. 1A and Methods). Live cells (sytox-negative) were isolated by FACS sorting, and scRNA-seq was conducted using the FACS-based method (Methods) [17]. After basic quality filtering, 1454, 1519, and 1466 Trypsin, TryPLE, and Liberase cells were obtained, respectively. The obtained data were visualized using UMAP (Fig. 1B). The cells were mainly separated into two clusters, and annotated as suprabasal or basal keratinocytes. Suprabasal keratinocytes exclusively expressed Krt1 and Krt10, which are well-known differentiation markers of suprabasal keratinocytes (Fig. 1C). Cells lacking Krt1/10, but expressing Krt5/14, Col17a1, and Trp63 were classified as basal keratinocytes (Fig. 1C).

Quality checks were performed to evaluate whether the choice of enzyme affected the quality of the scRNA-seq data. No significant differences in terms of the number of genes, universal molecular identifier (UMI) per cell, or the percentage of mitochondrial genes were observed, indicating that the data were of roughly the same quality (Fig. 2A–C). To further analyze the scRNA-seq data, the cells were colored according to the enzyme of choice for UMAP (Fig. 3A). Regardless of the choice of enzyme, both basal and suprabasal keratinocytes were recovered. However, the distribution of cells in UMAP differed depending on the choice of enzyme. Notably, the Liberase protocol enriched the suprabasal keratinocytes, whereas Trypsin and TrypLE were more favorable for enriching the basal keratinocytes (Fig. 3B). These data suggest that digestive enzymes tend to have a preference in terms of the recovery of cells from the neonatal mouse epidermis.

4. Discussion

Mouse models are widely used as an essential tool in skin research. The neonatal stage is the focal point for analyzing many skin diseases, underscoring the importance of optimizing methods for such analyses. In single-cell analyses, the isolation of individual cells from tissues is particularly crucial for obtaining high-quality data. In this study, three commonly used dissociation enzymes (Trypsin, TrypLE, and Liberase) were analyzed and compared using scRNA-seq, which revealed significant differences in the types of cells recovered depending on the enzyme used. The ratio of basal to suprabasal keratinocytes varied substantially. These findings indicate that the choice of the dissociation method can significantly influence scRNA-seq data and highlight the need for researchers to carefully select appropriate methods for specific studies.

The choice of enzymes for tissue dissociation had a significant impact on the scRNA-seq data. The use of Liberase enabled the recovery of a greater number of suprabasal cells. Suprabasal cells are strongly interconnected through tight junctions, which play a critical role in the skin's barrier function. It is possible that the robust cell-cell adhesion mediated by these tight junctions was not effectively disrupted by Trypsin or TrypLE. Liberase, which contains collagenase I, collagenase II, and thermolysin, may have the advantage of breaking down these tight junctions. However, caution is necessary when interpreting single-cell analyses because they primarily examine cell populations. The higher recovery of suprabasal cells with Liberase may be attributed to its inability to efficiently dissociate cells located near the basement membrane, resulting in the relative enrichment of suprabasal cells. Further research is required to develop more unbiased methods for analyzing the mouse neonatal epidermis to ensure comprehensive and representative data.

This study had some limitations. While three enzymatic dissociation methods were examined—Trypsin, TrypLE, and Liberase— other commonly used enzymes also warrant evaluation. Additionally, to address the challenges associated with enzymatic tissue dissociation methods such as those explored in this study, alternative approaches such as single-nucleus RNA sequencing (snRNA-seq), which analyzes isolated nuclei, have been actively developed in recent years. For single-cell analysis of the neonatal epidermis, it is important to evaluate whether single-cell or single-nucleus approaches are better suited for studying the epidermis.

Recently, various single-cell analysis techniques have been developed and are widely used in numerous fields, including development and disease studies. These methods often rely on the isolation of individual cells, highlighting the need for the development of more intact and unbiased techniques. Therefore, it is essential to optimize these methods for specific species, tissues, and developmental stages. In this study, enzymes commonly used for tissue dissociation were examined, and distinct characteristics of each enzyme were observed. The findings presented in this study provide an important foundation for the analysis of the mouse neonatal epidermis.

CRediT authorship contribution statement

Asaka Miura: Conceptualization, Formal analysis, Investigation, Visualization, Writing – original draft. **Tomomi Kitayama:** Formal analysis, Investigation, Visualization, Writing – original draft. **Yuya Ouchi:** Formal analysis, Investigation, Visualization, Writing – original draft. **Kotaro Saga:** Conceptualization, Supervision. **Takashi Shimbo:** Conceptualization, Supervision, Writing – original draft. **Katsuto Tamai:** Conceptualization, Supervision.

Data availability statement

The scRNA-seq data used in this study were deposited in the Gene Expression Omnibus (GEO) under accession number GSE283184.

Declaration of competing interest

K.T. is a scientific founder and received research funding from StemRIM Inc. K.T. and T.S. are StemRIM Inc. stockholders. Y.O., T.K., and K.T. are employees of StemRIM Inc.

The other authors declare no competing interests.

Acknowledgements

This study was supported by the JSPS KAKENHI [19H03682] and JSPS KAKENHI [22KJ2215].

References

[1] K.A.U. Gonzales, E. Fuchs, Skin and its regenerative powers: an alliance between stem cells and their niche, Dev. Cell 43 (11) (2017) 387–401.

[2] P. Gadre, P. Markova, M. Ebrahimkutty, Y. Jiang, F.M. Bouzada, F.M. Watt, Emergence and properties of adult mammalian epidermal stem cells, Dev. Biol. 515 (2024) 129–138.

[3] E. Candi, R. Schmidt, G. Melino, The cornified envelope: a model of cell death in the skin, Nat. Rev. Mol. Cell Biol. 6 (2005) 328–340.

[4] J.A. Segre, Epidermal barrier formation and recovery in skin disorders, J. Clin. Invest. 116 (2006) 1150–1158.

[5] L. Pulkkinen, J. Uitto, Mutation analysis and molecular genetics of epidermolysis bullosa, Matrix Biol. 18 (1999) 29–42.

[6] J. Uitto, G. Richard, Progress in epidermolysis bullosa: genetic classification and clinical implications, Am. J. Med. Genet. C Semin. Med. Genet. 131C (2004) 61–74.

[7] D.P. Kelsell, E.E. Norgett, H. Unsworth, M.-T. Teh, T. Cullup, C.A. Mein, P. J. Dopping-Hepenstal, B.A. Dale, G. Tadini, P. Fleckman, K.G. Stephens, V. P. Sybert, S.B. Mallory, B.V. North, D.R. Witt, E. Sprecher, A.E.M. Taylor, A. Ilchyshyn, C.T. Kennedy, H. Goodyear, C. Moss, D. Paige, J.I. Harper, B. D. Young, I.M. Leigh, R.A.J. Eady, E.A. O'Toole, Mutations in ABCA12 underlie the severe congenital skin disease harlequin ichthyosis, Am. J. Hum. Genet. 76 (2005) 794–803.

[8] B. Burja, D. Paul, A. Tastanova, S.G. Edalat, R. Gerber, M. Houtman, M. Elhai, K. Bürki, R. Staeger, G. Restivo, R. Lang, S. Sodin-Semrl, K. Lakota, M. Tomšič, M. P. Levesque, O. Distler, Ž. Rotar, M.D. Robinson, M. Frank-Bertoncelj, An optimized tissue dissociation protocol for single-cell RNA sequencing analysis of fresh and cultured human skin biopsies, Front. Cell Dev. Biol. 10 (2022) 872688.

[9] A. Broggi, C. Cigni, I. Zanoni, F. Granucci, Preparation of single-cell suspensions for cytofluorimetric analysis from different mouse skin regions, J. Vis. Exp. (2016) e52589.

[10] K. Sakamoto, S. Goel, A. Funakoshi, T. Honda, K. Nagao, Flow cytometry analysis of the subpopulations of mouse keratinocytes and skin immune cells, STAR Protoc 3 (2022) 101052.

[11] T.G. Hamilton, R.A. Klinghoffer, P.D. Corrin, P. Soriano, Evolutionary divergence of platelet-derived growth factor alpha receptor signaling mechanisms, Mol. Cell Biol. 23 (2003) 4013–4025.

[12] P.A. Joshi, P.D. Waterhouse, K. Kasaian, H. Fang, O. Gulyaeva, H.S. Sul, P. C. Boutros, R. Khokha, PDGFRα+ stromal adipocyte progenitors transition into epithelial cells during lobulo-alveologenesis in the murine mammary gland, Nat. Commun. 10 (2019) 1760.

[13] L. Madisen, T.A. Zwingman, S.M. Sunkin, S.W. Oh, H.A. Zariwala, H. Gu, L.L. Ng, R.D. Palmiter, M.J. Hawrylycz, A.R. Jones, E.S. Lein, H. Zeng, A robust and high-throughput Cre reporting and characterization system for the whole mouse brain, Nat. Neurosci. 13 (2010) 133–140.

[14] S. Papini, D. Cecchetti, D. Campani, W. Fitzgerald, J.C. Grivel, S. Chen, L. Margolis, R.P. Revoltella, Isolation and clonal analysis of human epidermal keratinocyte stem cells in long-term culture, Stem Cell. 21 (2003) 481–494.

[15] D. Correa-Gallegos, H. Ye, B. Dasgupta, A. Sardogan, S. Kadri, R. Kandi, R. Dai, Y. Lin, R. Kopplin, D.S. Shenai, J. Wannemacher, R. Ichijo, D. Jiang, M. Strunz, M. Ansari, I. Angelidis, H.B. Schiller, T. Volz, H.-G. Machens, Y. Rinkevich, CD201 + fascia progenitors choreograph injury repair, Nature 623 (2023) 792–802.

[16] Y.-T. Ho, T. Shimbo, E. Wijaya, T. Kitayama, S. Takaki, K. Ikegami, K. Miyashita, Y. Ouchi, E. Takaki, R. Yamamoto, Y. Kaneda, K. Tamai, Longitudinal single-cell transcriptomics reveals a role for serpina3n-mediated resolution of inflammation in a mouse colitis model, Cell Mol Gastroenterol Hepatol (2021), https://doi.org/10.1016/j.jcmgh.2021.04.004.

[17] J. Cao, J.S. Packer, V. Ramani, D.A. Cusanovich, C. Huynh, R. Daza, X. Qiu, C. Lee, S.N. Furlan, F.J. Steemers, A. Adey, R.H. Waterston, C. Trapnell, J. Shendure, Comprehensive single-cell transcriptional profiling of a multicellular organism, Science 357 (2017) 661–667.

[18] Illumina, Bcl2fastq and Bcl2fastq2 Conversion Software, 2017. https://emea.support.illumina.com/sequencing/sequencing_software/bcl2fastq-conversion-software.html.

[19] G.X.Y. Zheng, J.M. Terry, P. Belgrader, P. Ryvkin, Z.W. Bent, R. Wilson, S. B. Ziraldo, T.D. Wheeler, G.P. McDermott, J. Zhu, M.T. Gregory, J. Shuga, L. Montesclaros, J.G. Underwood, D.A. Masquelier, S.Y. Nishimura, M. Schnall-Levin, P.W. Wyatt, C.M. Hindson, R. Bharadwaj, A. Wong, K.D. Ness, L.W. Beppu, H.J. Deeg, C. McFarland, K.R. Loeb, W.J. Valente, N.G. Ericson, E.A. Stevens, J. P. Radich, T.S. Mikkelsen, B.J. Hindson, J.H. Bielas, Massively parallel digital transcriptional profiling of single cells, Nat. Commun. 8 (2017) 14049.

[20] A. Dobin, C.A. Davis, F. Schlesinger, J. Drenkow, C. Zaleski, S. Jha, P. Batut, M. Chaisson, T.R. Gingeras, STAR: ultrafast universal RNA-seq aligner, Bioinformatics 29 (2013) 15–21.

[21] Y. Hao, S. Hao, E. Andersen-Nissen, W.M. Mauck 3rd, S. Zheng, A. Butler, M.J. Lee, A.J. Wilk, C. Darby, M. Zager, P. Hoffman, M. Stoeckius, E. Papalexi, E.P. Mimitou, J. Jain, A. Srivastava, T. Stuart, L.M. Fleming, B. Yeung, A.J. Rogers, J. M. McElrath, C.A. Blish, R. Gottardo, P. Smibert, R. Satija, Integrated analysis of multimodal single-cell data, Cell 184 (2021) 3573–3587.e29.

[22] G. Yu, L.-G. Wang, Y. Han, Q.-Y. He, clusterProfiler: an R package for comparing biological themes among gene clusters, OMICS 16 (2012) 284–287.

[23] T. Wu, E. Hu, S. Xu, M. Chen, P. Guo, Z. Dai, T. Feng, L. Zhou, W. Tang, L. Zhan, X. Fu, S. Liu, X. Bo, G. Yu, clusterProfiler 4.0: a universal enrichment tool for interpreting omics data, Innovation 2 (2021) 100141.

[24] G.Y.E.H. Gao, Visualization of Functional Enrichment Result, Bioconductor, 2023. https://www.bioconductor.org/packages/release/bioc/html/enrichplot.html. (Accessed 17 July 2024).

[25] Plotly Technologies Inc, Plotly Python Open Source Graphing Library, 2015. https://plotly.com/python/. (Accessed 17 July 2024).

[26] H. Wickham, ggplot2: Elegant Graphics for Data Analysis, Springer-Verlag, New York, 2016.